Journal of Applied Fluid Mechanics, Vol. 9, No. 2, pp. 729-739, 2016.
Available online at www.jafmonline.net, ISSN 1735-3572, EISSN 1735-3645.
DOI: 10.18869/acadpub.jafm.68.225.21487

Analysis of MHD Williamson Nano Fluid Flow over a Heated Surface

S. Nadeem[1†] and S. T. Hussain[2]

[1]*Department of Mathematics, Quaid-I-AzamUniversity 45320, Islamabad 44000, Pakistan.*
[2]*DBS&H, CEME, National University of Sciences and Technology, Islamabad, Pakistan*

†*Corresponding Author Email: snqau@hotmail.com*

(Received September 12, 2013; accepted April 20, 2015)

ABSTRACT

In the present article Williamson nano fluid flow over a continuously moving surface is discussed when the surface is heated due to the presence of hot fluid under it. Governing equations have been developed and simplified using the suitable transformations. Mathematical analysis of various physical parameters is presented and the percentage heat transfer enhancement is discussed due to variation of these parameters. We employed Optimal homotopy analysis method to obtain the solution. It is presented that initial guess optimization will provide us one more degree of freedom to obtain the convergent and better solutions.

Keywords: **Nano** fluid; Convective heat transfer; Optimal homotopy analysis method (OHAM); Non-linearly moving surface.

NOMENCLATURE

a	stretching parameter
B	magnetic field (N/(mA))
b	body force (N)
Bi	Biot number
C	nanoparticles volumetric fraction
c	specific heat (J/kg K)
D_B	brownian diffusion coefficient (m²/s)
D_T	thermophoretic diffusion coefficient (m²/s)
E	electric field (N/C)
h	convective heat transfer coefficient (W/m² K)
I	identity tensor
J	current density (A/m²)
i,j	indexing variable
k	nano fluid thermal conductivity (W/m K)
M	magnetic parameter
n	stretching index
Nu	local Nusselt number
p	pressure (N/m²)
Pr	Prandtl number
Re	local Reynolds number
S	cauchy stress tensor (N/m²)
Sc	Schmidt number
Sh	local Sherwood number
T	temperature of fluid (K)
t	time (s)
u	horizontal component of velocity (m/s)
V	velocity vector (m/s)
v	vertical component of velocity (m/s)
x	distance along the plate
σ	electrical conductivity (S/m)
ν	kinematic viscosity (m²/s)
α	thermal diffusivity (m²/s)
ρ	density (kg/m³)
η	similarity variable
λ	non Newtonian Williamson parameter

subscripts

B	brownian motion
T	thermophoresis
∞	infinity
p	nano particles
w	wall
m	iteration number

1. INTRODUCTION

Nano fluid is the combination of simple fluid and nano sized particles uniformly suspended in the fluid. These nano sized particles can be metallic (Cu, Al, Hg, Ti, etc.) or non-metallic (ZnO, Al_20^3, TiO_2 and several other metallic oxides). Nano particles have advantage over micro size particles due to negligible effects of gravitational settling and cluster formation during flow. Fluids are widely used in heat transfer phenomenon due to their strong convection properties. Nano fluids got the attention of researchers and industrialists due to their better performance in heat transfer phenomenon. Several researchers

(Bang and Chang 2005; Suganthi and Rajan 2012; Kuznetsov 2011) have discussed the Nano fluid flow for various physical phenomenon by considering water as base fluid. But suspension of solid particles in water up to large percentage of its volume will change it from the Newtonian to non-Newtonian fluid. Also we know that several non-Newtonian fluids have better heat transfer properties as compared with water for e.g. liquid metals. So it's important to discuss the flow of non-Newtonian nano fluids due to their wide range use in industrial and chemical processes. Choi (1995) was the first one to use the term nano fluid due to nano sized particle suspension in fluid. He discussed that nano particles (due to their small size) are much better as compared to micro sized particles and their incorporation can reduce the cooling cost several times. Masuda *et al*. (1993) discussed the thermal conductivity enhancement due to addition of ultrafine particles in fluid. Buongiorno (2006) discussed the already presented mathematical models for nano fluid flow. He analyzed the possible effect of seven slip mechanisms on heat transfer enhancement and concluded that only Brownian motion and theromophoresis are the important slip mechanisms. He modeled the governing equations for the nano fluid flow. Nield and Kuzentsov (2009) discussed the thermal instability in a porous medium layer saturated by a nano fluid using the Buongiorno model. In another paper (2011), they discussed the double diffusive convection in a nano fluid flow. Nadeem and Lee (2012) obtained the analytical solutions for the boundary layer flow of a nano fluid over an exponentially moving surface. Khan and Pop (2010), numerically investigated the boundary layer flow of nano fluid past a stretching sheet. Recently Malvandi and Ganji (2014 a,b,c) discussed in detail the effect of Brownian motion and thermophoresis on the nano fluid flow in a microchannel.

The study of flow over a continuous moving surface is a popular area of research due to its enormous application in industrial manufacturing processes. Flows over continuously moving surface are widely discussed by researchers after the pioneering work of Sakiadis (1961). He first time modelled the boundary layer equations for the flow over a continuous moving surface which has been widely discussed afterwards (Ziabakhsh *et al*. 2010; Nadeem *et al*. 2012, 2013; Saleh *et al*. 2010). But many physical phenomenons involve the non-linear stretching for e.g. extrusion of plastic sheet, glass manufacturing etc. Cortell (2007) initiated the study of flows over non-linearly stretching surface. He numerically investigated the flow of viscous fluid over a non-linearly stretching surface. Raptis and Perdikis (2006) discussed the flow of viscous fluid over a non-linearly stretching surface in the presence of magnetic field. Abbasbandy and Ghehsareh (2012) presented the solutions for magnetohydrodynamic fluid over a non-linear stretching sheet with the help of Hankel-Pade method. Some studies of viscous nano fluid over non-linear stretching surface have been reported in literature (Rahman and Eltayeb 2013; Rana and Bhargava 2012; Hady *et al*. 2012), but very little attention has been given to the flow of non-Newtonian nano fluid. Therefore the present article discusses the flow of non-Newtonian nano fluid with convective boundary conditions. Convective boundary conditions are generalized as compared to constant surface temperature condition and have application in cooling systems and heat exchangers. Recently, Mansur and Ishak (2013) discussed the blasius flow for a copper water nano fluid with convective boundary conditions. They extended the work of Aziz (2009), who discussed the laminar flow of viscous fluid with convective boundary conditions. Makinde and Aziz (2011) investigated the boundary layer flow of nano fluid with convective boundary conditions. All of the aforementioned studies consider the viscous fluid with convective boundary condition.

Williamson fluid model describes the flow of shear thinning non-Newtonian fluids. This model was proposed by Williamson (1929) and later on used by several authors (Dapra and Scarpi 2007; Vasudev *et al*. 2012; Nadeem and Akbar 2010) to investigate fluid flow. We used Optimal Homotopy Analysis Method (OHAM) to solve the governing system of equation for Williamson nano fluid flow. OHAM is the refined version of Homotopy Analysis Method (HAM) Liao (2012). HAM has been widely used to solve the nonlinear differential equations (Malvandi *et al*. 2014 a,b; Abbasbandy 2007; Hayat and Qasim 2010; Shehzad *et al*. 2012). Recently Liao (2010) has suggested that it is better to use OHAM instead of HAM for better rate of convergence. He discussed different types of OHAM and suggested that it's better to use basic OHAM due to its computational efficiency. In OHAM discrete squared residual errors are optimized against the convergence control parameters. Fan and You (2013) discussed the global and step by step approaches to optimize the convergence control parameters. Nadjafi and Jafari (2011) compared Liao's optimal homotopy analysis method with the Niu's one-step optimal homotopy analysis method. They employed both techniques to obtain solution of linear Volterra integro-differential equations and integro-differential equation and concluded that Liao's optimal HAM has more accuracy to determine the convergence-control parameter than the one-step optimal HAM suggested by Niu and Wang (2010).

In the present article boundary layer equations for the

flow of MHD non-Newtonian Williamson nano fluid with convective boundary condition have been developed. Suitable transformations have been introduced to convert system of partial differential equations to the system of ordinary differential equations. The governing nonlinear coupled system of ordinary differential equations has been solved with the help of OHAM. In order to examine the validity of results they are compared with the numerical results. Effects of important physical parameters have been discussed through graphs and tables. To the best of author's knowledge no study has been reported for Williamson nano fluid over a non-linearly stretching surface with convective boundary condition.

2. MATHEMATICAL FORMULATION

We consider a steady two dimensional flow of an incompressible MHD Williamson nano fluid over a horizontal heated surface. Where x and y-axis are taken along horizontal and vertical direction respectively. So that nano fluid is confined to y > 0. The plate is stretched along x-axis with the velocity ax^n, where a > 0 is stretching parameter and n is the stretching index. It is assumed that the surface is heated due to convection of hot fluid below the surface. A space varying magnetic field B(0, *B(x)*, 0) is applied along the transverse direction of flow see Fig.l. The fluid is assumed to be slightly conducting, so that the magnetic Reynolds number is much less than unity and hence the induced magnetic field is negligible in comparison to the applied magnetic field. The general transport equations for nano fluid are (Boungiorono 2006)

$$\operatorname{div}\mathbf{V} = 0, \tag{1}$$

$$\rho\frac{d\mathbf{V}}{dt} = \operatorname{div}\mathbf{S} + \mathbf{b}, \tag{2}$$

$$\rho c\left(\frac{\partial T}{\partial t} + \mathbf{V}\cdot\nabla T\right) = \nabla\cdot k\nabla T + \rho_p c_p\left(D_B\nabla\varphi\cdot\nabla T + D_T\frac{\nabla T\cdot\nabla T}{T_\infty}\right), \tag{3}$$

$$\frac{\partial C}{\partial t} + \mathbf{V}\cdot\nabla C = \nabla\cdot\left(D_B\nabla C + D_T\frac{\nabla T}{T_\infty}\right), \tag{4}$$

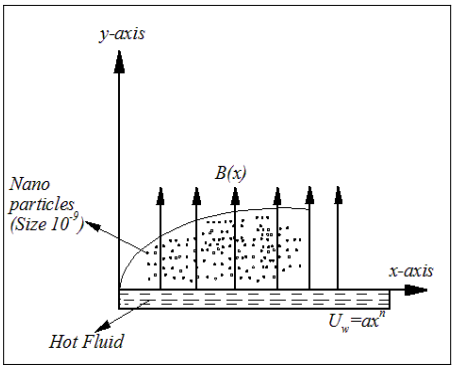

Fig. 1. Geometry of the problem.

where in steady state the velocity vector is given by **V**(u(x, y), v(x, y), 0), ρ is nano fluid density and p_p is nano particles density, **S** is Cauchy stress tensor, **b** is body force vector, *c* and c_p are heat capacities of nano fluid and nano particles respectively, *T* is temperature, *k* is nano fluid thermal conductivity, $D_B$is Brownian diffusion coefficient, *C* is nano particles volumetric fraction, $D_T$is thermophoretic diffusion coefficient and T_∞ is the ambient fluid temperature. For Williamson fluid model Cauchy stress tensor **S** is defined as

$$\mathbf{S} = -p\mathbf{I} + \boldsymbol{\tau}, \tag{5}$$

$$\boldsymbol{\tau} = [\,\mu_\infty + \frac{(\mu_0 - \mu_\infty)}{1-\Gamma\dot{\gamma}}\,]\mathbf{A}_1, \tag{6}$$

in above equations $\boldsymbol{\tau}$ is extra stress tensor, μ_0 is limiting viscosity at zero shear rate and μ_∞ is limiting viscosity at infinite shear rate, $\Gamma > 0$ is a time constant, $\mathbf{A}_1$ is the first Rivlin-Erickson tensor and $\dot{\gamma}$ is defined as follows [28-30]

$$\dot{\gamma} = \sqrt{\frac{1}{2}\,\pi}, \qquad \pi = trace(\mathbf{A}_1^2). \tag{7}$$

Here, we considered the case for which $\mu_\infty = 0$ and $\Gamma\dot{\gamma} < 1$. Thus $Eq.(6)$ can be written as

$$\boldsymbol{\tau} = [\,\frac{\mu_0}{1-\Gamma\dot{\gamma}}\,]\mathbf{A}_1, \tag{8}$$

or by using binomial expansion we get

$$\boldsymbol{\tau} = \mu_0[1+\Gamma\dot{\gamma}]\mathbf{A}_1. \tag{9}$$

The interaction of magnetic field and velocity will give rise to the Lorentz force $\mathbf{J}\times\mathbf{B}$ defined in Eq.(10), in which **J** is the current density and σ is the electrical conductivity. In the absence of electric field $\mathbf{E} = \mathbf{0}$.

$$\mathrm{J} = \sigma(\mathrm{E} + \mathrm{V}\times\mathrm{B}) \tag{10}$$

Since we have considered the steady state velocity so all the derivatives w.r.t are zero. Making use of $Eqs.(5),(9)$ and (10) in $Eqs.(1-4)$ the two dimensional boundary layer equations governing the flow are given by

$$\frac{\partial u}{\partial x} + \frac{\partial v}{\partial y} = 0, \tag{11}$$

$$u\frac{\partial u}{\partial x} + v\frac{\partial u}{\partial y} = \nu\frac{\partial^2 u}{\partial y^2} + \sqrt{2}\nu\Gamma\frac{\partial u}{\partial y}\frac{\partial^2 u}{\partial y^2} - \frac{\sigma B^2(x).u}{\rho} \tag{12}$$

$$u\frac{\partial T}{\partial x} + v\frac{\partial T}{\partial y} = \alpha\frac{\partial^2 T}{\partial y^2} + \frac{\rho_p c_p}{\rho c}\left(D_B\frac{\partial C}{\partial y}\frac{\partial T}{\partial y} + \frac{D_T}{T_\infty}\left(\frac{\partial T}{\partial y}\right)^2\right), \tag{13}$$

$$u\frac{\partial C}{\partial x} + v\frac{\partial C}{\partial y} = D_B\frac{\partial^2 C}{\partial y^2} + \frac{D_T}{T_\infty}\frac{\partial^2 T}{\partial y^2}, \tag{14}$$

where $u(x, y)$ and $v(x, y)$ are horizontal and

vertical components of velocity, v is kinematic viscosity and α is nano fluid thermal diffusivity. The magnetic field is chosen as $B(x) = B_{\circ}\sqrt{x^{n-1}}$. The corresponding boundary conditions to the flow problem are

$$u = U_w = ax^n;\ v = 0\ ;\ -k\frac{\partial T}{\partial y} = h(T_f - T),\ C = C_w \text{ at } y = 0,$$
$$u \to 0\ ;\ T = T_\infty, C = C_\infty \text{ as } y \to \infty. \qquad (15$$

In boundary conditions k is thermal conductivity, T_f is the temperature of the hot fluid and h is the convective heat transfer coefficient. Introducing the following transformations in above equations

$$u = ax^n f'(\eta), v = -\sqrt{\frac{a(n+1)\nu x^{n-1}}{2}}\left[f(\eta) + \frac{n-1}{n+1}\eta f'(\eta)\right],$$
$$\eta = \sqrt{\frac{a(n+1)x^{n-1}}{2\nu}}y, \theta = \frac{T - T_\infty}{T_w - T_\infty},\ \varphi = \frac{C - C_\infty}{C_w - C_\infty}. \qquad (16$$

With the help of above transformations, *Eq.*(11) is identically satisfied and *Eqs.*(12) to (14) along with boundary conditions (15) take the following form

$$f''' - \frac{2n}{n+1}f'^2 + ff'' + \lambda f'' f''' - Mf' = 0, \qquad (17)$$

$$\theta'' + \Pr f\theta' + \frac{Nc}{Le}\varphi'\theta' + \frac{Nc}{LeNbt}\theta'^2 = 0, \qquad (18)$$

$$\varphi'' + Scf\varphi' + \frac{1}{Nbt}\theta'' = 0, \qquad (19)$$

The corresponding boundary conditions and the non-dimensional parameter are

$$f = 0,\ f' = 1,\ \theta' = -Bi(1-\theta),\ \varphi = 1 \quad \text{at } \eta = 0,$$
$$f' = 0,\ \theta = 0,\ \varphi = 0 \quad \text{as } \eta \to \infty. \qquad (20$$

Mathematically, *Sc* can be written as

$$Sc = \frac{\upsilon}{D_B} = \frac{\alpha}{D_B}\frac{\upsilon}{\alpha} = Le\,\Pr. \qquad (21)$$

With the help of *Eq.*(21) , *Eq.*(19) can be written as

$$\varphi'' + Le\,\Pr f\varphi' + \frac{1}{Nbt}\theta'' = 0. \qquad (22)$$

$\lambda = \Gamma\sqrt{\frac{a^3(n+1)x^{3n-1}}{\nu}}$ (non Newtonian Williamson parameter),

$\Pr = \frac{\upsilon}{\alpha}$ (momentum diffusivity/nano fluid thermal diffusivity),

$Le = \frac{\alpha}{D_B}$ (nano fluid thermal diffusivity/Brownian diffusivity),

$Sc = \frac{\upsilon}{D_B}$ (momentum diffusivity/Brownian diffusivity).

$M = \frac{2\sigma B_{\circ}^2}{\rho a(n+1)}$ (Magnetic parameter)

$\frac{Bi}{\sqrt{\mathrm{Re}_x}} = \frac{hx}{k}\sqrt{\frac{2}{n+1}}$ (Surface convection parameter or reduced Biot number)

$Nc = \frac{\rho_p c_p}{\rho c}(C_w - C_\infty)$ (nano particles heat capacity/nano fluid heat capacity),

$Nbt = \frac{D_B T_\infty (C_w - C_\infty)}{D_T (T_w - T_\infty)}$ (Brownian diffusivity/ thermophoretic diffusivity).

Since we are interested in the study of heat transfer enhancement, so it is better to introduce the effects of thermal diffusivity in nano particles equation with the help of Le and $\Pr$. Also it will enhance the coupling effects of heat and nano particles equation. Finally, Eqs. (17), (18) and (22) form the non-dimensional system of equation with corresponding boundary conditions given in (20) . For $\lambda = 0$, problem reduces to the one for Newtonian nano fluid and for $D_B = D_T = 0$ in *Eq.*(12), heat equation reduces to the classical boundary layer heat equation in the absence of viscous dissipation. Physical quantities of interest for present study are local Nusselt number Nu and local Sherwood number Sh .

$$Nu = \frac{-x}{T_w - T_\infty}\left.\frac{\partial T}{\partial y}\right|_{y=0},\ Sh = \frac{-x}{C_w - C_\infty}\left.\frac{\partial C}{\partial y}\right|_{y=0}, \qquad (23$$

or by introducing the transformations (16) , we get

$$\frac{Nu}{\sqrt{\mathrm{Re}_x}} = -\sqrt{\frac{n+1}{2}}\theta'(0),\ \frac{Sh}{\sqrt{\mathrm{Re}_x}} = -\sqrt{\frac{n+1}{2}}\varphi'(0), \qquad (24$$

where $\mathrm{Re}_x = \frac{U_w x}{\upsilon}$ is local Reynolds number. Physical parameters will be discussed later in the results section.

3. HOMOTOPY BASED SOLUTION TECHNIQUE

HAM is a strong analytic technique to solve linear and non-linear, ordinary and partial differential equations. HAM was developed by Liao (2003), This technique is better than the perturbation techniques as it can be equally applied to weak and strong nonlinear problems. It is also independent of small and large physical parameter restriction. The advantage of HAM lies in the choice of convergence control parameter according to the given set values of input parameters. It provides a

way to check and adjust the convergence of obtained solution with the help of auxiliary parameters and base functions. To obtain the homotopy based solutions, we choose two sets of initial guess defined by (23) , ε is a simple constant its value will be determined in the optimization section. This initial guess reduces to the most commonly used initial guess $f_0(\eta) = 1 - \exp(-\eta)$, when $\varepsilon = 1$. In the result section we will show that $\varepsilon = 1$ is not the best value, but it is better to optimize ε for the best possible value.

$$f_0(\eta) = \varepsilon + (1-2\varepsilon)\exp(-\eta) - (1-\varepsilon)\exp(-2\eta),$$
$$\theta_0(\eta) = \frac{Bi}{Bi+1}\exp(-\eta),$$
$$\varphi_0(\eta) = \exp(-\eta),$$

)(25

$$\mathrm{L}_{\mathrm{f}}(\mathrm{f}) = \frac{\mathrm{d}^3\mathrm{f}}{\mathrm{d}\eta^3} - \frac{\mathrm{df}}{\mathrm{d}\eta},$$
$$\mathrm{L}_{\theta}(\theta) = \frac{\mathrm{d}^2\theta}{\mathrm{d}\eta^2} + \frac{\mathrm{d}\theta}{\mathrm{d}\eta}, \quad (26)$$
$$\mathrm{L}_{\varphi}(\varphi) = \frac{\mathrm{d}^2\varphi}{\mathrm{d}\eta^2} + \frac{\mathrm{d}\varphi}{\mathrm{d}\eta},$$

Due to space constraint the detailed HAM procedure is not discussed here. The detailed HAM procedure can be followed from [32]. We can calculate any order approximation for $m = 1, 2, 3...$ with the help of Mathematica.

3.1 Optimal Convergence Control Parameters

It is noteworthy that our solutions $f(\eta), \theta(\eta)$ and $\varphi(\eta)$ will contain unknown convergence control (auxiliary) parameters (h_f, h_θ, h_φ). To find out the optimal values of convergence control parameters we define the exact squared residuals at the m[th] order approximation as follows

$$\mathcal{E}_m^f = \int_0^\infty \left\{ N_f[\sum_{i=0}^m f_i(\eta)] \right\}^2 d\eta, \quad (27)$$

$$\mathcal{E}_m^\theta = \int_0^\infty \left\{ N_\theta[\sum_{i=0}^m f_i(\eta), \sum_{i=0}^m \theta_i(\eta), \sum_{i=0}^m \varphi_i(\eta)] \right\}^2 d\eta, \quad (28)$$

$$\mathcal{E}_m^\varphi = \int_0^\infty \left\{ N_\varphi[\sum_{i=0}^m f_i(\eta), \sum_{i=0}^m \theta_i(\eta), \sum_{i=0}^m \varphi_i(\eta)] \right\}^2 d\eta, \quad (29)$$

and

$$\mathcal{E}_m^t = \mathcal{E}_m^f + \mathcal{E}_m^\theta + \mathcal{E}_m^\varphi, \quad (30)$$

where $\mathcal{E}_m^t$ is the total squared residual error and $\mathcal{E}_m^f$ $\mathcal{E}_m^\theta, \mathcal{E}_m^\varphi$ are the corresponding individual errors at m[th] iteration. In above equations $\mathrm{N_f}$, $\mathrm{N_\theta}$, $\mathrm{N_\varphi}$ denotes the left hand side of the equations (17), (18) and (19) at the m[th] order deformation respectively. It is obvious that quickly $\mathcal{E}_m^t$ approaches to zero, faster the corresponding solution converges. Thus at m[th] iteration the optimal values of convergence control parameters are given by the minimum of $\mathcal{E}_m^t$, corresponding to the set of these equations

$$\frac{\partial \mathcal{E}_m^t}{\partial h_f} = \frac{\partial \mathcal{E}_m^t}{\partial h_\theta} = \frac{\partial \mathcal{E}_m^t}{\partial h_\varphi} = \frac{\partial \mathcal{E}_m^t}{\partial \varepsilon} = 0. \quad (31)$$

The total squared residual error defined by $Eq.(30)$ takes too much CPU time to calculate the error even if the order of approximation is not very high. Thus to increase the computational efficiency we define the discrete squared residual error (as defined by Liao [38]) at the m[th] iteration by

$$E_m^f \approx \frac{1}{N+1}\sum_{j=0}^N \left\{ N_f[\sum_{i=0}^m f_i(\eta_j)] \right\}^2, \quad (32)$$

$$E_m^\theta \approx \frac{1}{N+1}\sum_{j=0}^N \left\{ N_\theta[\sum_{i=0}^m f_i(\eta_j), \sum_{i=0}^m \theta_i(\eta_j), \sum_{i=0}^m \varphi_i(\eta_j)] \right\}^2,$$

)(33

$$E_m^\varphi \approx \frac{1}{N+1}\sum_{j=0}^N \left\{ N_\varphi[\sum_{i=0}^m f_i(\eta_j), \sum_{i=0}^m \theta_i(\eta_j), \sum_{i=0}^m \varphi_i(\eta_j)] \right\}^2,$$

)(34

where $\eta_j = j\Delta\eta,\ \Delta\eta = 0.5$ and $N = 20$ in above equations. The total discrete squared residual error is defined as

$$E_m^t = E_m^f + E_m^\theta + E_m^\varphi.$$
$$\frac{\partial E_m^t}{\partial h_f} = \frac{\partial E_m^t}{\partial h_\theta} = \frac{\partial E_m^t}{\partial h_\varphi} = \frac{\partial E_m^t}{\partial \varepsilon} = 0. \quad (35)$$

In present paper total discrete squared residual error approach is used to obtain optimal convergence control parameters. In order to obtain the local optimal convergence control parameters, we directly employ the minimize command in computational software Mathematica.

4. RESULTS AND DISCUSSION

In homotopy analysis method, the convergence control parameters are chosen from the range of values, obtained through h-curves. After plotting the h-curves we randomly choose the values of convergence control parameter from the convergence region. But with the help of Optimal Homotopy, we precisely choose the best possible values of the convergence control parameters.

4.1 Optimal Values of Convergence Parameters

In this section the Optimal values of convergence control parameters are shown when $Bi = 5, \mathrm{Pr} = 2, Nc = 0.5, Nbt = 2, Le = 2, \lambda = 0.2, n = 0.5, M = 0.8$ Table.1 shows the total discrete squared residual

Table 1 Average squared residual errors at different order of approximation

m	h_f	h_θ	h_φ	ε	E_m^f	E_m^θ	E_m^φ	E_m^t
1	-1.25	-0.74	-3.79	0.74	5.98×10^{-4}	9.69×10^{-4}	6.97×10^{-3}	8.54×10^{-3}
5	-0.81	-0.55	-0.99	0.73	1.51×10^{-6}	9.47×10^{-6}	7.18×10^{-5}	8.28×10^{-5}
7	-0.69	-0.59	1.17	0.70	6.05×10^{-7}	1.98×10^{-7}	6.97×10^{-6}	7.78×10^{-6}
9	-0.66	-0.60	-1.27	0.72	4.30×10^{-8}	2.67×10^{-9}	3.35×10^{-7}	3.80×10^{-7}

error at different order of approximation. We split table.1 into two sections one for the case $\varepsilon = 1$ (most commonly used case) and other when ε is optimized instead of setting its particular value.

Table 2 Local Optimal convergence control parameters at different order of approximation

m	h_f	h_θ	h_φ	$E_m^t(\varepsilon=1)$
1	-1.23	-0.80	0.07	2.61×10^{-2}
5	-0.69	-0.35	0.93	4.71×10^{-4}
7	-0.67	-0.35	-3.05	1.12×10^{-4}
9	-0.63	-0.35	1.80	3.49×10^{-5}

m	h_f	h_θ	h_φ	ε	E_m^t
1	–1.25	–0.74	–3.79	0.74	8.54×10^{-3}
5	–0.81	–0.55	–0.99	0.73	8.12×10^{-5}
7	–0.69	–0.59	1.17	0.70	7.56×10^{-6}
9	–0.66	–0.60	–1.27	0.72	3.75×10^{-7}

For the present study we found that total squared residual error can be reduced significantly if we optimize initial guess by introducing arbitrary parameter. So we will use the optimized value of ε instead of choosing $\varepsilon = 1$. Table.1 also gives the optimal values of convergence parameters at different order of approximations. These optimal values are used to obtain the discrete squared residual errors at different order of approximation see Table.2. It is observed that the average squared residual error and total squared residual error decrease as the number of iterations increased. This assures that better solutions are obtained at higher order approximations. We choose, 9th iteration set of optimal values to plot figures and draw tables in the coming sections. Results will be similar if we choose optimal convergence parameters value from 9th or any higher order approximation.

4.2 Plots and Tables

Fig.2 is drawn to examine the effect of magnetic field on the nano fluid velocity. We observe that velocity profile decrease with increase in M. Eq. (10) involves the cross product of velocity vector and magnetic field vector, it will give rise to Lorentz force which is perpendicular to the velocity vector and magnetic field vector. This force will act as a resistive force to the fluid flow which will ultimately slow down the fluid motion. It is also clear that the momentum boundary layer thickness decreases with the increase in magnetic parameter M. Fig.3 shows that temperature increases due to the increase in M. Nano fluid contains the nano size particles whose motion is affected by the applied magnetic field. These particles act as the energy carrier to the fluid causing the increase in nano fluid temperature. M is zero, when no external magnetic field is applied. We can also see that thermal boundary layer is increasing with the increase in M.

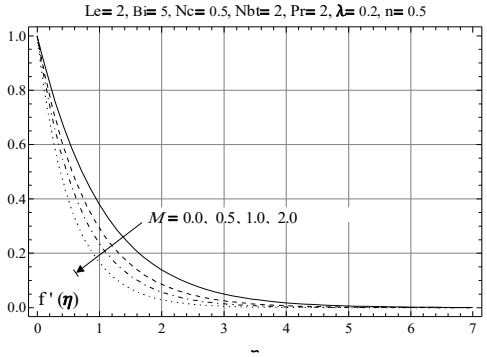

Fig. 2. Velocity profile against M.

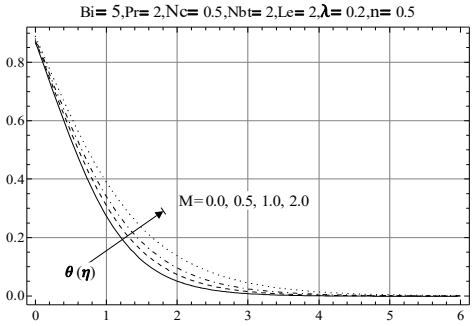

Fig. 3. Temperature profile against M.

Fig.4 shows that the temperature profile against η for different values of Biot number Bi. We can see that the temperature at wall is varying with Bi because of convective boundary conditions. When Bi approaches to infinity the temperature boundary condition at wall reduces to the case of constant wall temperature. Thus convective boundary conditions are more generalized as compare to the constant wall temperature condition. The graph also depicts that as the Bi approaches to 100, θ attain the constant wall temperature condition $\theta(0) = 1$.

Biot number is the ratio of the convection at the surface to the conduction within the surface. Thus large Biot number implies stronger convection at the surface and small Biot number implies stronger conduction within the surface. Temperature graph against Bi also predicts this behavior, the fluid temperature increases with the increase in Bi. Also thermal boundary layer increases with the increase in Bi.

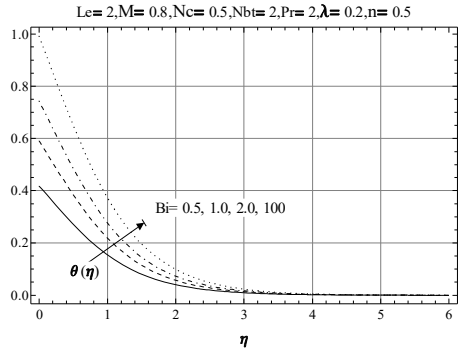

Fig. 4. Temperature profile against Bi.

Figs.5 and 6 demonstrate the effects of Lewis number Le and diffusivity ratio Nbt, on the temperature profile when other parameters are kept constant. Temperature profile as well as thermal boundary layer thickness decrease with the increase in Le. Le and Nbt cannot be chosen equal to zero because Le appears in the denominator of the Eq. (18) and Nbt appears in the denominator of both Eq. (18) and (22). Physically Le cannot equal to zero since it is ratio of thermal diffusivity to Brownian diffusion. Buongiorno (2006) defined the parameter Nbt to discuss the relative effect of Brownian diffusion to thermophoretic diffusion, we followed the same parameter. It is observed that temperature profile and thermal boundary layer decrease with increase in Nbt. when Brownian diffusivity is very large as compared to thermophoretic diffusivity, temperature profile only shows very small variation.

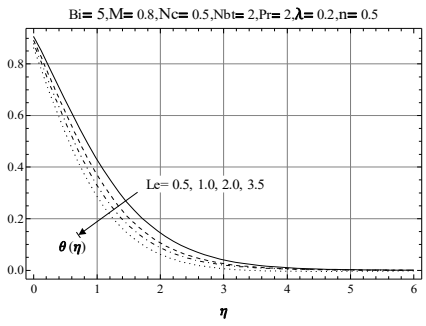

Fig. 5. Temperature profile against Le.

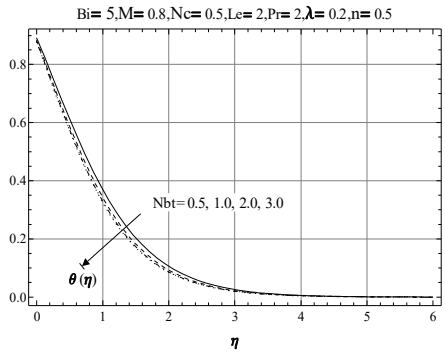

Fig. 6. Temperature profile against Nbt.

Fig.7 describes the effect of heat capacities ratio Nc on the temperature profile. It is observed that temperature and thermal boundary layer thickness increases with the increase in Nc. If we look at the definition of Nc, it is ratio of heat capacity of nano particles and nano fluid. Usually the specific heat c_p of nano particles is less than that of base fluid because typically specific heat of solid is less than that of liquids. So addition of solid particles will decrease the specific heat of base fluid, hence temperature profile decrease. Fig.8 shows that the temperature and thermal boundary layer thickness decreases with the increase in Prandtl number Pr. As we know Pr controls the relative thickness of momentum and thermal boundary layer. Large Pr means smaller thermal boundary layer and larger momentum boundary layer.

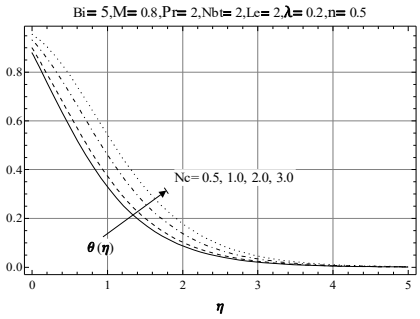

Fig. 7. Temperature profile against Nc.

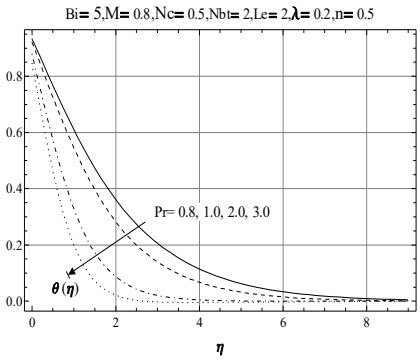

Fig. 8. Temperature profile against Pr.

Figs. 9-13 are drawn to examine the effects of important parameters on the nano particles volumetric fraction. Although some parameters are not directly involved in the nano particles volumetric fraction equation, but there effects are appearing due to the coupling of Eqs.(18) and (22). Eq. (22) is second order equation in both θ and φ. So value of Nbt will play the dominant rule when effects of parameters involved in θ are discussed for φ. Fig.9 shows the variation of nano particles volumetric fraction against Bi. The nano particles volumetric fraction increases with the increase in Bi. Since φ is equal to 1 at wall so its value remains fixed for different values of Bi while θ (0) was varying with Bi values (see Fig.4).

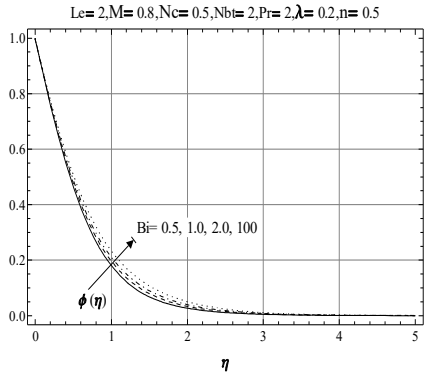

Fig. 9. Nano particles volumetric fraction against Bi

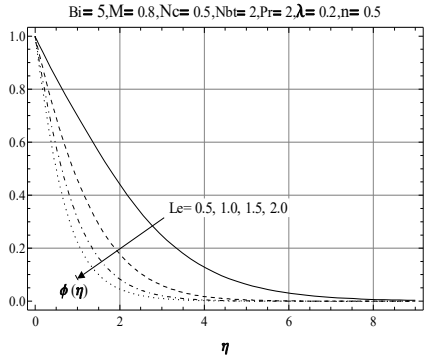

Fig. 10. Temperature profile against Le.

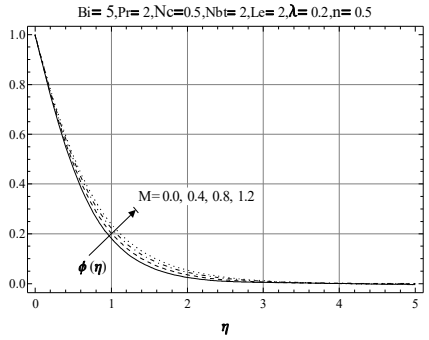

Fig. 11. Temperature profile against M.

It is noticed that φ decreases with the increase in Le and decreases with the increase in M (see Figs.10 and 11). The concentration boundary layer thickness decreases quickly as Le increase from 0.5 to 1. When the value of Le is less than 1, it implies Brownian diffusions have larger value than the thermal diffusion. Large Brownian diffusion will create larger penetration depth for concentration boundary layer which can be seen from Fig.10 for Le=0.5. Concentration boundary layer increases with the increase in M as seen in Fig. 11. When the value of M increases it excites fluid particles motion which will diffuses quickly into the neighboring fluid layers due to the enhanced Brownianmotion.

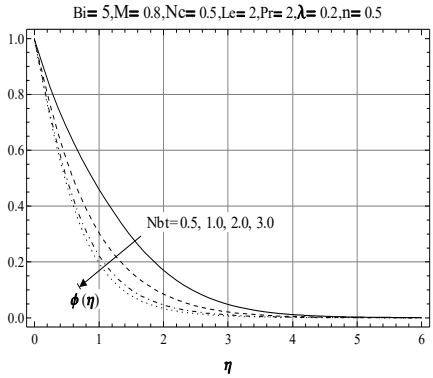

Fig. 12. Nano particles volumetric fraction against Nbt.

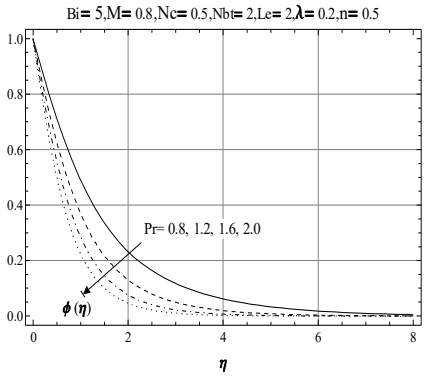

Fig. 13. Nano particles volumetric fraction againt Pr.

Figs.12 and 13 shows that φ decrease with the increase in Nbt and Pr. Since the Brownian and thermophoretic diffusion both cause the dispersion of particles across the boundary layer, thus the concentration profile decrease with the increase in Nbt across the flow field. Its effects on the concentration profile are more prominent as compared to the temperature profile due to the dominance of mass diffusion of nanoparticles. Nadeem and Haq (2014) have shown that concentration profile decreases with the increase in Prandtl number up to certain value of η and decrease afterwards. This effect is removed if product of Le and Pr is introduced instead of Sc in the nano particles equation and graph shows uniformly decreasing behavior against Pr throughout the boundary layer.

Tables.3 and 4 are drawn to examine the effects of important parameters on the local Nusselt and Sherwood numbers respectively. In order to compare the analytical results with numerical results, we used built in Maple 16 algorithm to obtain numerical solution for the boundary value problem. It is found that numerical results are in good comparison with the analytic results up to three decimal places. It is observed that the reduced Nusselt number ($Nu/\sqrt{Re}$) decreases with the increase in M, when other parameters are kept fixed while it increases with the increase in Pr. As the value of Pr increases from 0.8 to 2.0,reduced Nusselt number increases by 83%.

Table 3 Values of $-\sqrt{\frac{n+1}{2}}\theta'(0)$.

M	Pr	Nc	Le	Nbt	Bi	OHAM	Numerical
0	2.0	0.5	2.0	2.0	5.0	0.5658	0.5659
0.8						0.5185	0.5185
1.0						0.5086	0.5086
0.8	0.8	0.5	2.0	2.0	5.0	0.2833	0.2836
	1.6					0.4525	0.4526
	2.0					0.5185	0.5185
0.8	2.0	0.5	2.0	2.0	5.0	0.5185	0.5185
		1.0				0.4300	0.4301
		1.5				0.3530	0.3530
0.8	2.0	0.5	0.8	2.0	5.0	0.4436	0.4436
			1.5			0.4972	0.4972
			2.0			0.5185	0.5185
0.8	2.0	0.5	2.0	0.8	5.0	0.4912	0.4913
				1.5		0.5123	0.5123
				2.0		0.5185	0.5185
0.8	0.8	0.5	2.0	2.0	0.1	0.0758	0.0758
					0.2	0.1347	0.1347
					1.0	0.3533	0.3533
					10	0.5502	0.5502
					50	0.5783	0.5783

It is noticed that increasing the value of Nc decreases the wall temperature gradient. When Nc value is increased from 0.5 to 1.0, value of reduced Nusselt number is decreased by 17.06% and for the next 0.5 increase in Nc, it is decreased by 17.9%. So reduced Nusselt number decreases more quickly for greater than 1 value of Nc in comparison to less than 1 values. Le is important parameter due to involvement of thermal diffusivity and Brownian diffusion coefficient. It is observed that reduced Nusselt number shows increasing behavior with the increase in Le. When Le=0.5, the value of reduced Nusselt number is 0.4004. It can be calculated that when the thermal diffusivity is increased from half the value of Brownian diffusion coefficient to twice the value of Brownian diffusion coefficient, reduced Nusselt number shows an enormous increase of 29%. When the value of Nbt is increased beyond 1, Brownian diffusion coefficient becomes dominant over the thermophoretic diffusion coefficient. This effects is visible in Table.3, reduced Nusselt number shows increasing behavior with the increasing value of Nbt. Due to convective boundary condition Bi is the important parameter involved in heat transfer. We computed reduced Nusselt number for several values of Bi to examine the effect of Bi on heat transfer when values are less than and greater than 1. When Bi is increased from 0.1 to 0.2, reduced Nusselt number is increased by 77.7%. For the next 0.8 increase in Bi value, reduced Nusselt number is increased by 162.2%. As Bi is increased from 1.0 to 10, reduced Nusselt number is increased by 55.7%. For the large increase in Bi from 10-50, reduced Nusselt number just shows an increase of 5.1%. After examining the effects of Bi on heat transfer, we can conclude that over all heat transfer rate increases with the increase in Bi. Increase in reduced Nusselt number is extremely significant for small values of Bi less than 1 (specifically about 0.1) and this increase starts reducing as Bi is increased beyond 1 and specifically 10.

Table.4 shows the variation in reduced Sherwood number (Sh/√Re) against M, Pr, Nc, Le and Nbt. Reduced Sherwood number decrease with the increase in M. When value of M is increased from 0 to 1, values of reduced Nusselt number decrease by 10.1% while value of reduced Sherwood number decrease by 9.2%. So M has more effect on wall temperature gradient as compared to wall concentration gradient. Reduced Sherwood number shows increasing trend with the increase in Pr and Nc. From Table.3 and 4, it is noticed that Nc has opposite effects on the reduced Nusselt number and Sherwood number. Le shows the increasing effect on reduced sherwood number. Reduced Sherwood number is increased by 108% as Le value is increased from 0.8 to 2.0. It can be calculated that when Le is equal to 1.3 the value of reduced Sherwood number is -0.7183. For the increase of 0.5 in Le (0.8-1.3), reduced Sherwood number is increased by 50.6% and for the same increase of 0.5 (1.5-2.0), it is increased by 23.6%. This shows that reduced Sherwood number is greatly affected by the value of Le. It is also observed that reduced Sherwood number increases with the increase in Nbt.Table.5 is drawn to compare the values of wall temperature gradient for different types of fluid when n=1/2. It is noticed from the table that wall temperature gradient decrease as fluid is changed from viscous to Williamson MHD nano fluid when some of the parameters have fixed values as mentioned in front of them. By Fourier law of heat conduction $q = -k\,\frac{\partial T}{\partial y}$, k has inverse relation with the temperature gradient for fixed heat flux. Therefore, Williamson MHD nano fluid has higher thermal conductivity than all other fluids mentioned in Table.5.

Table 4 Values of $-\sqrt{\frac{n+1}{2}}\varphi'(0)$

M	Pr	Nc	Le	Nbt	HAM	Numerical
0	2.0	0.5	2.0	2.0	1.0746	1.0744
0.8					0.9920	0.9920
1.0					0.9751	0.9747
0.8	1.2	0.5	2.0	2.0	0.7063	0.7060
	1.6				0.8575	0.8574
	2.0				0.9920	0.9920
0.8	2.0	0.5	2.0	2.0	0.9920	0.9920
		1.0			1.0273	1.0271
		1.5			1.0569	1.0567
0.8	2.0	0.5	0.8	2.0	0.4767	0.4767
			1.5		0.8025	0.8024
			2.0		0.9920	0.9920
0.8	2.0	0.5	2.0	0.8	0.8188	0.8187
				1.5	0.9510	0.9510
				2.0	0.9920	0.9920

5. CONCLUDING REMARKS

In present article flow of MHD Williamson nano fluid over a non-linearly stretching surface with convective boundary conditions has been discussed in detail. The governing PDE's are transformed to coupled system of nonlinear ODE's and OHAM is employed to solve the resulting system of ODE's. OHAM results have been compared with numerical

results. The main findings of the paper are as follows

- Better values of total squared residual errors are obtained by optimizing the initial guess.
- OHAM results are in good comparison with the numerical results.
- Mathematically it is appropriate to introduce product of Lewis and Prandtl instead of Schmidt number in the nano particles volumetric fraction equation.
- In the neighborhood of 0.1 a small incremental increase in reduced Biot number shows enormous increase in the reduced Nusselt number.
- Nc has opposite effect on the modified Nusselt and modified Sherwood number.
- Thermal conductivity of MHD Williamson nano fluid is higher than that of simple Williamson fluid.

Table 5Values of wall temperature gradient for different fluids

Fluid type	-θ'(0)
Viscous fluid (λ=0, M=0, Pr=2)	0.7822
Williamson fluid (λ=0.3, M=0, Pr=2)	0.7722
MHD viscous fluid (λ=0, M=0.8, Pr=2)	0.7259
MHD Williamson fluid (λ=0.3, M=0.8, Pr=2)	0.7056
Williamson nano fluid (λ=0.3, M=0, Pr=2, Nc=0.5, Le=2, Nbt=2)	0.6501

ACKNOWLEDGEMENT

This research was supported by the Higher Education Commission of Pakistan (PhD indigenous scheme PIN no. 112-21674-2PS1-576).

REFERENCES

Abbasbandy, S. (2007). The application of homotopy analysis method to solve a generalized HirotaSatsuma coupled KdV equation.*Physics Letters A* 361(6), 478-483.

Abbasbandy, S. and H. R. Ghehsareh (2012). Solutions of the magnetohydrodynamic flow over a nonlinear stretching sheet and nano boundary layers over stretching surfaces.*International Journal for Numerical Methods in Fluids* 70, 1324-1340.

Aziz, A. (2009). A similarity solution for laminar thermal boundary layer over a flat plate with a convective surface boundary condition. *Communications in Nonlinear Science and Numerical Simulation* 14, 1064-1068.

Bang, I. C. and S. H. Chang (2005). Boiling heat transfer performance and phenomena of Al_20^3—water nano-fluids from a plain surface in a pool, *International Journal of Heat and Mass Transfer* 48(12), 2407-2419.

Buongiorno, J. (2006). Convective transport in nanofluids.*Journal of Heat Transfer*128, 240-250.

Choi, S. (1995). *Enhancing Thermal Conductivity of Fluids With nanoparticles in Developments and Applications of non-Newtonian Flows*.D. A.Siginer and H. P. Wang eds., ASME. 66, 99-105.

Cortell, R. (2007). Viscous flow and heat transfer over a nonlinearly stretching sheet, *Applied Mathematics and Computation* 184, 864-873.

Dapra, I. and G. Scarpi (2007). Perturbation solution for pulsatile flow of a non-Newtonian Williamson fluid in a rock fracture, *International Journal of Rock Mechanics and Mining Sciences* 44, 271-278.

Fan, T. and X. You(2013). Optimal homotopy analysis method for nonlinear differential equations in the boundary layer, *Numerical Algorithms* 62, 337-354.

Hady, F. M., F. S. Ibrahim, S. M. Abdel-Gaied and M. R. Eid(2012). Radiation effect on viscous flow of a nanofluid and heat transfer over a nonlinearly stretching sheet.*Nanoscale Research Letters* 7, 229.

Hayat, T. and M. Qasim(2010). Influence of thermal radiation and Joule heating on MHD flow of a Maxwell fluid in the presence of thermophoresis.*International Journal of Heat and Mass Transfer* 53, 4780-4788.

Khan, W. A. and I. Pop(2010). Boundary-layer flow of a nanofluid past a stretching sheet.*International Journal of Heat and Mass Transfer* 53, 2477-2483.

Kuznetsov, A.V. (2011). Nanofluid bioconvection in water-based suspensions containing nanoparticles and oxytactic microorganisms: oscillatory instability. *Nanoscale Research* Letters 6, 100.

Liao, S. (2003).*Beyond Perturbation: Introduction to the Homotopy Analysis Method*, Chapman and Hall/CRC99-102.

Liao, S. (2010). An optimal homotopy-analysis approach for strongly nonlinear differential equations.*Communications in Nonlinear Science and Numerical Simulation* 15, 2003-2016.

Liao, S. (2012).*Homotopy Analysis Method in Nonlinear Differential Equations*. Springer &Higher Education Press, Heidelber.

Makinde,O.D and A. Aziz(2011). Boundary layer flow of a nanofluid past a stretching sheet with a convective boundary condition.*International Journal of Thermal Sciences*50(7),1326-1332.

Malvandi, A.and D.D. Ganji(2014). Brownian motion and thermophoresis effects on slip flow of alumina/water nanofluid inside a circular microchannel in the presence of a magnetic field.*International Journal of Thermal Sciences* 84, 196-206.

Malvandi, A., F. Hedayati and M. R. H. Nobari (2014).An HAM Analysis of Stagnation-Point Flow of a Nanofluid over a Porous Stretching Sheet with Heat Generation.*Journal of Applied Fluid Mechanics* 7(1), 135-145.

Malvandi, A. and D.D. Ganji (2014). Magnetic field effect on nanoparticles migration and heat transfer of water/alumina nanofluid in a channel.*Journal of Magnetism and Magnetic Materials* 362, 172-179.

Malvandi, A., F. Hedayati and M. R. H. Nobari (2014).An Analytical Study on Boundary Layer Flow and Heat Transfer of Nanofluid Induced by a Non-Linearly Stretching Sheet.*Journal of Applied Fluid Mechanics* 7(2), 375-384.

Malvandi, A. and D.D. Ganji (2014). Mixed convective heat transfer of water/alumina nanofluid inside a vertical microchannel.*Powder Technology* 263, 37-44.

Mansur, S. and A. Ishak(2013). Blasius flow for a copper-water nanofluid with a convective boundary condition.*AIP Conference Proceedings*583, 15-22.

Masuda, H., A. Ebata, K. Teramae and N. Hish-inuma(1993). Alteration of Thermal Conductivity and Viscosity of Liquid by Dispersing Ultra-Fine Particles.*Netsu Bussei*7(4), 227-233.

Nadeem.S, C. Lee(2012). Boundary layer flow of nanofuid over an exponentially stretching sur-face.*Nanoscale Research letters* 7, 94.

Nadeem, S. and N. S AkbarNumerical solutions of peristaltic flow of Williamson fluid with radi-ally varying MHD in an endoscope.*International Journal for Numerical Methods in Fluids* 66(2), 212-220.

Nadeem, S., R. Mehmood and N. S. Akbar (2013). Non-orthogonal stagnation point flow of a nano non-Newtonian fluid towards a stretching surface with heat transfer.*International Journal of Heat and Mass Transfer* 57(2), 679-689.

Nadeem, S., R. U. Haq and C. Lee(2012). MHD flow of a Casson fluid over an exponentially shrinking sheet.*Scientica Iranica* 19(6), 1550-3.

Nadeem, S., Rizwan Ul Haq and Z.H. Khan (2014). Numerical study of MHD boundary layer flow of a Maxwell fluid past a stretching sheet in the presence of nanoparticles.*Journal of the Taiwan Institute of Chemical Engineers* 45(1), 121-126.

Nadjafi, J. S. and H. S. Jafari(2011). Comparison of Liao's optimal HAM and Niu's one-step optimal HAM for solving integro-differential equations.*Journal of Applied Mathematics & Bioinformatics*1(2), 85-98.

Nield, D.A. and A.V. Kuznetsov(2009). Thermal instability in a porous medium layer saturated by a nanofluid.*International Journal of Heat and Mass Transfer* 52, 5796-5801.

NieldD, A. and A.V. Kuznetsov(2011). The onset of double-diffusive convection in a nanofluid layer.*International Journal of Heat and Fluid Flow* 32, 771-776.

Niu, Z. and C. Wang (2010). A one-step optimal homotopy analysis method for nonlinear differential equations.*Communications in Nonlinear Science and Numerical Simulation* 15, 2026-2036.

Rahman, M. M. and I.A. Eltayeb(2013). Radiative heat transfer in a hydromagnetic nanofluid past a nonlinear stretching surface with convective boundary condition. *Meccanica*48, 601-615.

Rana, P. and R. Bhargava (2012). Flow and heat transfer of a nanofluid over a nonlinearly stretching sheet: A numerical study.*Communications in Nonlinear Science and Numerical Simulation* 17(1), 212-226.

Raptis, A. and C. Perdikis (2006). Viscous flowover a non-linearly stretching sheet in the presence of a chemical reaction and magnetic field. *International Journal of Non-Linear Mechanics* 41,527- 529.

Sakiadis, B. C.(1961). Boundary layer behavior on continuous solid flat surfaces.*American Institute of Chemical Engineers Journal* 726-28.

Salleh, M. Z., R. Nazar and I. Pop(2010). Boundary layer flow and heat transfer over a stretching sheet with Newtonian heating.*Journal of the Taiwan Institute of Chemical Engineers*41(6), 651-655.

Shehzad, S. A., A. Alsaedi and T. Hayat(2012). Three-dimensional flow of Jeffery fluid with convective surface boundary conditions.*International Journal of Heat and Mass Transfer* 55(15-16), 3971-3976.

Suganthi, K.S. and K.S. Rajan(2012). Temperature induced changes in ZnO water nanofluid: Zeta potential size distribution and viscosity profiles.*International Journal of Heat and Mass Transfer* 55(25-26), 7969-7980.

Vasudev, C., U. R. Rao, M. V. S Reddy and G. P. Rao(2010). Peristaltic Pumping of Williamson fluid through a porous medium in a horizontal channel with heat transfer.*American Journal of Scientific and Industrial Research* 1(3), 656-666.

Williamson, R.V. (1929). The flow of pseudoplastic materials.*Industrial & Engineering Chemistry* 21(11), 1108-1111.

Ziabakhsh, Z., G. Domairry, H. Bararnia and H. Babazadeh(2010). Analytical solution of flow and diffusion of chemically reactive species over a non-linearly stretching sheet immersed in a porous medium.*Journal of the Taiwan Institute of Chemical Engineers*41(1), 22-28.